Determinants of heart rate variability in obstructive sleep apnea syndrome during wakefulness and sleep

J. A. Jo, A. Blasi, E. Valladares, R. Juarez, A. Baydur and M. C. K. Khoo

AJP - Heart 288:1103-1112, 2005. First published Oct 7, 2004; doi:10.1152/ajpheart.01065.2003

AJP - Heart and Circulatory Physiology publishes original investigations on the physiology of the heart, blood vessels, and lymphatics, including experimental and theoretical studies of cardiovascular function at all levels of organization ranging from the intact animal to the cellular, subcellular, and molecular levels. It is published 12 times a year (monthly) by the American Physiological Society, 9650 Rockville Pike, Bethesda MD 20814-3991. ISSN: 0363-6135, ESSN: 1522-1539. Visit our website at http://www.the-aps.org/.

Am J Physiol Heart Circ Physiol 288: H1103–H1112, 2005.
First published October 7, 2004; doi:10.1152/ajpheart.01065.2003.

Determinants of heart rate variability in obstructive sleep apnea syndrome during wakefulness and sleep

J. A. Jo,[1] A. Blasi,[1] E. Valladares,[1] R. Juarez,[2] A. Baydur,[2] and M. C. K. Khoo[1]

Departments of [1]Biomedical Engineering and [2]Medicine, University of Southern California, Los Angeles, California

Submitted 4 December 2003; accepted in final form 4 October 2004

Jo, J. A., A. Blasi, E. Valladares, R. Juarez, A. Baydur, and M. C. K. Khoo. Determinants of heart rate variability in obstructive sleep apnea syndrome during wakefulness and sleep. *Am J Physiol Heart Circ Physiol* 288: H1103–H1112, 2005. First published October 7, 2004; doi:10.1152/ajpheart.01065.2003.—Heart rate variability (HRV) is mediated by at least three primary mechanisms: *1*) vagal feedback from pulmonary stretch receptors (PSR), *2*) central medullary coupling between respiratory and cardiovagal neurons (RCC), and *3*) arterial baroreflex (ABR)-induced fluctuations. We employed a noninvasive experimental protocol in conjunction with a minimal model to determine how these sources of HRV are altered in obstructive sleep apnea syndrome (OSAS). Respiration, heart rate, and blood pressure were monitored in eight normal subjects and nine untreated OSAS patients in relaxed wakefulness and stage 2 and rapid eye movement sleep. A computer-controlled ventilator delivered inspiratory pressures that varied randomly from breath to breath. Application of the model to the corresponding subject responses allowed the delineation of the three components of HRV. In all states, RCC gain was lower in OSAS patients than in normal subjects ($P < 0.04$). ABR gain was also reduced in OSAS patients ($P < 0.03$). RCC and ABR gains increased from wakefulness to sleep ($P < 0.04$). However, there was no difference in PSR gain between subject groups or across states. The findings of this study suggest that the adverse autonomic effects of OSAS include impairment of baroreflex gain and central respiratory-cardiovascular coupling, but the component of respiratory sinus arrhythmia that is mediated by lung vagal feedback remains intact.

baroreflex sensitivity; respiratory sinus arrhythmia; cardiovascular control; system identification

OBSTRUCTIVE SLEEP APNEA SYNDROME (OSAS) is characterized by repetitive episodes of upper airway collapse during sleep. The obstruction of inspiratory airflow results in asphyxia and subsequent vigorous efforts to breathe, leading eventually to transient arousal and restoration of upper airway patency. These dramatic events exert a profound acute influence on the cardiovascular system. It is believed that long-term exposure to episodic apnea and arousal constitutes an independent risk factor for systemic hypertension, heart failure, myocardial infarction, and stroke (10, 33, 34). In particular, the evidence suggests that abnormal autonomic control is likely a key factor in the causal pathway linking OSAS to these cardiovascular diseases (36, 42).

Time-domain and spectral analyses of heart rate variability (HRV) have been employed as noninvasive methods of assessing cardiovascular autonomic function in patients with OSAS (40, 28). However, these analyses yield information that reflects only the net effect of all the factors that contribute to heart rate control, thus providing little insight into which of the underlying physiological mechanisms are most affected by the abnormality. For instance, fluctuations in blood pressure can affect heart rate through stimulation of the arterial and cardiac baroreceptors (24). This mechanism is believed to be a key determinant of the 0.1-Hz periodicity frequently observed in the heart rate power spectrum in humans. Fluctuations in blood pressure entrained by respiration contribute to some extent to the oscillation more commonly known as "respiratory sinus arrhythmia" (RSA). However, in this case, at least two other mechanisms have also been shown to play an important role (14). Animal studies have pointed to a direct central link between the respiratory and cardioregulatory rhythm-generating neurons in the medulla, so that vagal cardioinhibitory motoneurons of the nucleus ambiguus, which influence heart rate, receive a powerful inhibitory synaptic input throughout inspiration and are excited in the early expiratory or postinspiratory phase (35). A third suggested mechanism for RSA is vagal feedback from PSR, which modulates efferent outflow to the sinus node (2). In their classic studies on anesthetized dogs, Anrep and colleagues (2, 3) used specific denervation of the lung to determine the importance of vagal feedback from lung stretch receptors and tested the importance of the central link of respiratory to cardiovascular regulation by using a cross-cerebral circulation technique to cause hypocapnia-induced apnea (in the recipient dog) without the need for augmented lung stretch. Either of these mechanisms acting alone was shown to be capable of producing a significant RSA in the anesthetized dog. In a study on normal humans and patients who had undergone lung or heart transplantation, Taha et al. (38) showed an obligatory role for lung vagal feedback in mediating RSA but concluded that, in the intact human, central and baroreflex modulation of RSA are also important. Thus different relative contributions from these mechanisms could yield the same magnitude of RSA.

Recently, we introduced a new noninvasive approach that provides a more precise assessment of autonomic function in patients with OSAS (7, 17). This approach combines an experimental protocol, in which a randomly modulated breathing sequence is used to induce fluctuations in heart rate and blood pressure with a computational model that allows estimation of the temporal relations between pairs of these signals. The experimental protocol presents the advantage of allowing the study of OSAS patients during wakefulness and sleep. The computational model enables HRV to be partitioned into a component directly correlated with respiration and a component representing arterial baroreflex (ABR)-mediated effects, thus allowing a less biased estimation of the ABR dynamics. In

Address for reprint requests and other correspondence: M. C. K. Khoo, Biomedical Engineering Dept., DRB-140, Univ. of Southern California, Los Angeles, CA 90080-1451 (E-mail: khoo@bmsr.usc.edu).

The costs of publication of this article were defrayed in part by the payment of page charges. The article must therefore be hereby marked "*advertisement*" in accordance with 18 U.S.C. Section 1734 solely to indicate this fact.

the present study, we have extended this model to include a more complete characterization of the mechanisms involved in RSA. More specifically, we have divided the respiratory-correlated contribution into two components: one representing the respiratory-cardiac neural coupling and the other representing the effect of vagal feedback from the PSR. As in our previous work (7, 17), it was assumed that the various interactions among the cardiorespiratory variables involved in the modulation of heart rate could be described by a linear, time-invariant, stationary parametric model.

Through the application of a novel experimental protocol in conjunction with a mathematical model of HRV, we sought *1*) to estimate and quantify the dynamics of the three main physiological mechanisms involved in the control of HRV, i.e., vagal lung stretch reflex, central cardiorespiratory coupling, and ABR; and *2*) to determine how these underlying mechanisms of autonomic control of HRV are altered by OSAS as well as by changes in wake-sleep state.

METHODS

Experimental protocol and instrumentation. Nine untreated patients with moderate to severe OSAS (apnea-hypopnea index = 44.1 ± 2.8 h^{-1}) and eight normal controls participated in overnight sleep studies. All subjects were male except for one female in the control group. Age was not significantly different between the two groups: 44.9 ± 2.8 and 50.1 ± 2.0 yr for OSAS patients and controls, respectively. However, body mass index was significantly higher in the OSAS patients (39.7 ± 4.2 vs. 28.4 ± 1.2 kg/m^2, $P < 0.05$). All subjects were normotensive and were free of diabetes, significant cardiac arrhythmia, congestive heart failure, and lung disease. Informed consent was obtained before each study. The protocol for the studies was approved by the University of Southern California Institutional Review Board.

Each subject was connected via nasal mask to a computer-controlled bilevel pressure ventilator (model S/T-D 30, Respironics, Pittsburgh, PA). Measurements of mask pressure (P_{mask}) and airflow ($\dot{Q}$) were obtained from the detachable control panel of the S/T-D ventilator. $\dot{Q}$ was electronically integrated in inspiratory and expiratory phases to obtain the instantaneous lung volume (V) relative to passive functional residual capacity. Consistent with a previous report (11), we found in initial tests that the tidal volumes derived from the ventilator volume monitor were highly correlated ($r > 0.97$, $P = 0.0001$) with corresponding readings obtained from a reference pneumotachometer (model 3700, Hans Rudolph, Kansas City, MO). A chin strap was used to keep the mouth closed during sleep, preventing leakage or inspiration through the mouth. Because some degree of continuous positive airway pressure (CPAP) was applied in all subjects, continuous monitoring of P_{mask} allowed us to detect abrupt or unusual changes in baseline pressure that could indicate leaks through the mouth.

Blood pressure was monitored continuously from one wrist using a noninvasive arterial tonometer (model 7000, Colin Medical Instruments, San Antonio, TX). Electrocardiogram, arterial O_2 saturation, central and occipital electroencephalogram, chin electromyogram, left and right electrooculogram, and nasal thermistor were also monitored. All signals were sampled at 200 Hz. During sleep in the OSAS patients, CPAP of 8–15 cmH_2O was applied to eliminate all obstructive apneas (defined as episodes of zero $\dot{Q}$ lasting ≥10 s) and significant hypopnea (defined as periods >10 s duration in which the nasal thermistor signal was reduced to <50% of its magnitude during unobstructed breathing and arterial O_2 saturation decreased by >4%). A minimal CPAP of 2–3 cmH_2O was applied during wakefulness in both groups. In the control subjects, CPAP was maintained at this minimal level during sleep.

During the 10-min test protocol, the ventilator was set to assist-control, bilevel ventilation mode. Here, the subject was allowed to breathe at his own respiratory rate, but the inspiratory pressure was switched randomly breath to breath between CPAP and CPAP + 5 cmH_2O. Expiratory pressure was kept constant at CPAP. With the use of this experimental setup, tidal volume was modulated from breath to breath without the need for voluntary control by the subject. This allowed the test protocol to be applied during sleep.

After one or two trials to minimize subject anxiety during wakefulness, the test protocol was applied at least three times in each sleep-wake state. Test sequences in which arousals or outright awakening occurred were terminated and were not repeated until the subject returned to a stable sleep state. Sleep stages were scored according to conventional criteria (31).

Data analysis. R-R intervals (RRI) and systolic and diastolic blood pressure (SBP and DBP) were deduced beat to beat and resampled at 2 Hz using the Berger algorithm (8). Very-low-frequency oscillatory behavior or baseline drift was observed in some of the datasets. These nonstationarities were removed by detrending the datasets before applying spectral analysis and modeling. The detrending procedure consisted of first fitting a fifth-order polynomial to the signals and then removing this curvilinear trend from the time series. The power spectrum of the subtracted trend was visually examined to verify that the detrending process had little effect on frequencies >0.04 Hz. After detrending, spectral analysis of RRI, DBP, and SBP was performed using an autoregressive modeling approach described previously (17). The respiratory signals were also resampled at 2 Hz, so that each respiratory value would be synchronized with the corresponding resampled RRI, SBP, and DBP values.

Model. On the basis of our knowledge of the underlying physiology (14, 24), fluctuations in heart rate, respiration, and blood pressure are assumed to be interrelated through the closed-loop control scheme (Fig. 1). For instance, apart from the direct mechanical effects of intrathoracic pressure changes, fluctuations in blood pressure are due in part to changes in cardiac output resulting from variations in heart rate as well as sympathetically driven variations in peripheral resistance. The focus of this study is limited to the other portion of the closed-loop model that accounts for HRV (Fig. 1). Fluctuations in RRI are decomposed into four components. The first three components correspond to the autonomically mediated mechanisms mentioned earlier: *1*) vagal feedback from PSR, represented in this model by the coupling between fluctuations in V and RRI, *2*) central medullary coupling between respiratory and cardiovagal neurons (RCC), represented in this model by the coupling between fluctuations in respiratory muscle pressure (P_{mus}) and RRI, and *3*) ABR-mediated fluctuations, represented also in this model by the interaction between blood pressure and RRI. The fourth component encompasses all other influences not explained by the baroreflex or the two respiratory-related components, such as changes in venous return during breathing and changes in chemoreceptor feedback.

A linear autoregressive model with triple exogenous inputs was employed to estimate the impulse responses and transfer functions of the three components of the model schematized in Fig. 1. The change in RRI from the mean at time t [$\Delta RRI(t)$] was related to weighted combinations of past values of ΔRRI, changes in P_{mus} (ΔP_{mus}), changes in lung volume (ΔV), and changes in SBP (ΔSBP), as given by the following difference equation

$$\Delta RRI(t) = -\sum_{i=1}^{P} a_i \Delta RRI(t-i) + \sum_{j=0}^{q} b_j \Delta V(t-j-D_{PSR}) + \sum_{k=0}^{m} c_k \Delta P_{mus}(t-k-D_{RCC}) + \sum_{l=0}^{r} d_l \Delta SBP(t-l-D_{ABR}) + W_{RRI}(t) \quad (t = 1,\ldots,N) \quad (1)$$

where D_{PSR}, D_{RCC}, and D_{ABR} are the delays associated with the corresponding mechanisms, $W_{RRI}(n)$ represents the variability of RRI

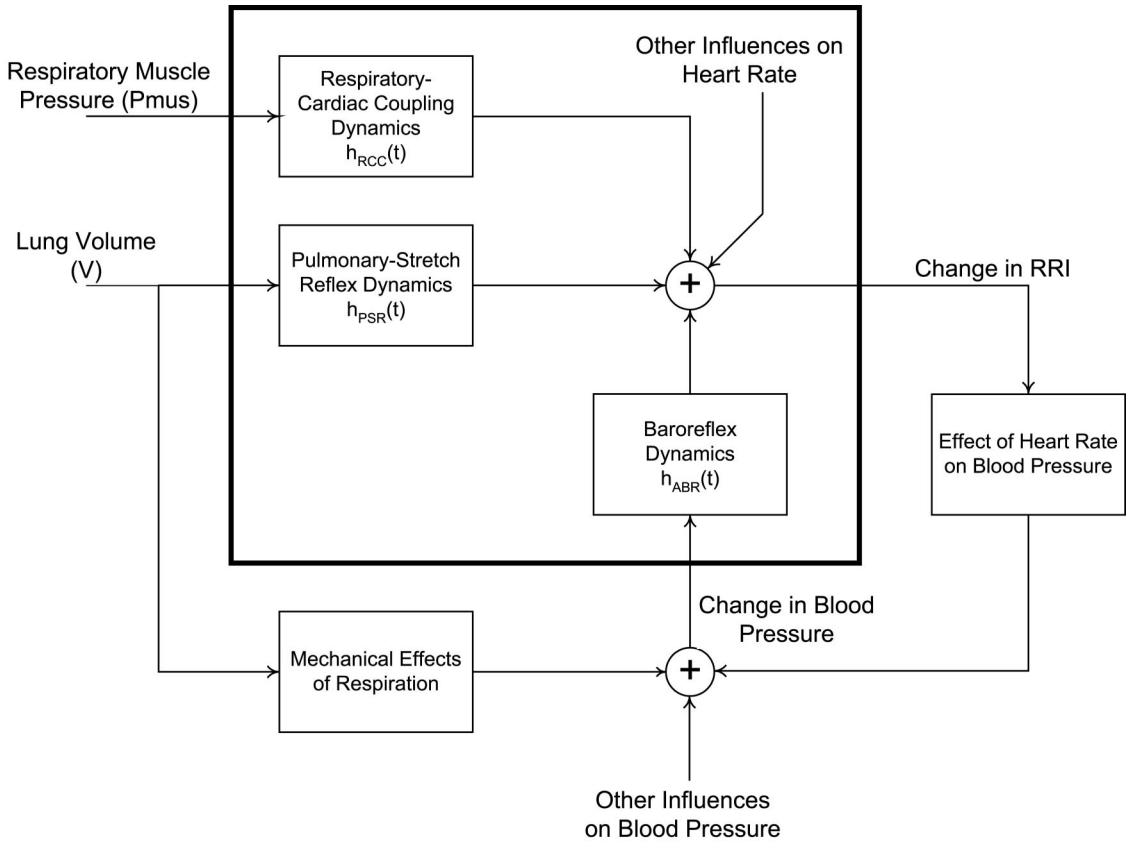

Fig. 1. Schematic block diagram of major physiological mechanisms that contribute to heart rate and blood pressure regulation. Components circumscribed by the box (bold lines) constitute the mathematical model employed in the study. Fluctuations on R-R interval (RRI) are assumed to be produced by pulmonary-stretch reflex (PSR), central respiratory-cardiac autonomic coupling (RCC), arterial baroreflex (ABR), and other extraneous influences. Dynamics of each mechanism are represented by their corresponding impulse response functions: $h_{PSR}(t)$, $h_{RCC}(t)$, and $h_{ABR}(t)$.

not explained by the model, a_i, b_j, c_k, and d_l represent unknown constant coefficients that need to be estimated from the data, and N is the total number of data points used in the analysis.

It is imperative to note that the system under study operates in a closed loop (Fig. 1), so that changes in heart rate can subsequently affect SBP through changes in cardiac output. In general, this condition, in which the model input is dependent on its output, can lead to erroneous parameter estimates when conventional analysis techniques are employed. To circumvent this problem, we formulated the model equations in the time domain so that "causality" constraints could be imposed, i.e., the model output was constrained mathematically to be dependent on only past values of the inputs. Previous studies employed similar methodologies that essentially allow the closed loop to be "opened" computationally (4, 7, 12, 17, 27, 41).

A delay of ≥0.5 s was assumed for D_{ABR}, the latency of the baroreflex impulse response. Physiologically based constraints were also imposed on the respiratory-related delays. Several previous studies on humans and animal preparations have noted that, during the average breathing cycle, heart rate begins accelerating in the last segment of the preceding expiratory phase (14, 18). Therefore, the model was allowed to adopt negative values of D_{RCC}. On the other hand, data from subjects who were passively ventilated suggest that, in this case, V precedes or is roughly in synchrony with RRI (38). Thus, in this case, V should precede RRI (or be almost synchronous with it). As such, the range of D_{PSR} was restricted to positive values close to zero. For each combination of delays, least-squares minimization was employed to estimate the unknown coefficients in *Eq. 1*. As well, for each combination of delays, a measure of the quality of fit, known as the minimum description length (MDL), was computed as follows (32)

$$\mathrm{MDL} = \log(J_R) + \frac{\text{total no. of parameters} \times \log(N)}{N} \qquad (2)$$

where J_R is the variance of the residual errors between the measured data and the predicted RRI. Note that MDL decreases as J_R decreases but increases with increasing model order. Selection of the "optimal" candidate model was based on a global search for the minimum MDL; in addition, this optimal solution had to satisfy the condition that the cross-correlations between the residual errors and past values of the three inputs [$\Delta V(t)$, $\Delta P_{mus}(t)$, and $\Delta SBP(t)$] were statistically indistinguishable from zero.

With use of this model, it was possible to estimate the impulse response functions, $h_{ABR}(t)$, $h_{PSR}(t)$, and $h_{RCC}(t)$, which characterize the gains and temporal properties of the baroreflex, PSR, and central-coupling mechanisms, respectively (Fig. 1): $h_{ABR}(t)$ quantifies the time course of the change in RRI resulting from an abrupt 1-mmHg increase in SBP, $h_{PSR}(t)$ quantifies the time course of the fluctuation in RRI associated with a very rapid inspiration and expiration of 1 liter of air, and $h_{RCC}(t)$ quantifies the time course of the fluctuation in RRI associated with an abrupt 1-cmH_2O increase in P_{mus}. In linear systems theory, the impulse response provides a complete characterization of the dynamic properties of the system in question, because the response of this system to any arbitrary input can be predicted by mathematically convolving the input with the impulse response (20). Each of the impulse response functions, $h_{ABR}(t)$, $h_{PSR}(t)$, and $h_{RCC}(t)$, was calculated by setting the associated input to unity at $t = 0$ and zero at all

other times, setting all other inputs and $W_{RRI}(t)$ to zero, and using *Eq. 1* to compute the resulting RRI response. Once the impulse response functions were estimated, it was also possible to compute the relative contributions of each of the three mechanisms to the overall predicted ΔRRI by convolving each impulse response with the corresponding input sequence. The ratio of the variance of the resulting convolved signal (representing the portion of the predicted ΔRRI explained by the corresponding input) divided by the variance of the overall predicted ΔRRI (obtained when the 3 inputs were included together) was taken as an index to quantify the relative contribution of each mechanism.

To quantify the strength of each mechanism (PSR, ABR, and RCC) on the modulation of HRV, two indexes representing the gain of each interaction were computed. *1*) The impulse response magnitudes (IRM) were calculated as the difference between the maximum and minimum values of the estimated impulse responses. *2*) The dynamic gains (DG) were estimated by first taking the Fourier transform of the impulse responses to obtain transfer functions and then calculating the average of transfer function gains between 0.04 and 0.45 Hz. This range covers the span of frequencies pertinent to HRV. The dynamic characteristics (e.g., response time) of each mechanism were also quantified from the impulse response by computing the delay or latency (D_{PSR}, D_{RCC}, or D_{ABR}) and the duration between start of the impulse response and its first major peak or valley (T_{peak}).

Estimation of P_{mus}. The respiratory rhythm-generating neurons in the medulla control phrenic activity, which, in turn, drives the respiratory muscles. Our model assumes, as previous physiological studies have suggested, a direct central link between these respiratory neurons and cardioregulatory neurons in the medulla, which, in turn, modulate heart rate. Because respiratory neural activity is not directly measurable in humans, P_{mus} was chosen to represent central respiratory drive. P_{mus} was deduced from $\dot{Q}$ and mask pressure (P_{mask}) signals using the following equation (26)

$$P_{mus} = R\dot{Q} + EV - P_{mask} \quad (3)$$

The first term on the right-hand side of *Eq. 3* represents the pressure used to overcome the resistance (R) of the respiratory system, whereas the second term represents the pressure associated with respiratory elastance (E). Previous studies have demonstrated that postinspiratory P_{mus} can persist for up to 70% of the time of expiration in anesthetized normal subjects (6) and in anesthetized patients with kyphoscoliosis, in whom respiratory elastance is markedly increased (5). Because E is also increased in OSAS patients, it is expected that postinspiratory P_{mus} also persists in a manner similar to that in normal subjects. So, on the basis of the previous findings, it is expected that postinspiratory braking is probably present to a similar degree in the OSAS and control groups and would reduce the variability in both groups to a roughly equal degree and, thus, would not contribute to major differences in the ABR, RCC, or PSR functions. Under this assumption, in the present study, expiration was taken to be entirely passive to make the computations and interpretations as simple as possible.

To calculate P_{mus}, it was necessary to estimate the respiratory mechanics parameters, R and E. R was estimated using a pulse technique (26). Brief pressure pulses, with amplitude of 5 cmH_2O and duration of 500 ms, were applied at randomly selected breaths through computer control of the inspiratory pressure level of the ventilator. Each pulse was delivered at the beginning of inspiration, when the elastic recoil of the respiratory system is least. To calculate R, the increase in pressure above continuous positive airway pressure (CPAP) during the pulse was divided by the peak increase in flow elicited by the pulse. This procedure was applied before the delivery of each test protocol. Estimates of R were based on the average to at least five responses.

E was estimated as follows. At end expiration on a randomly selected breath, an abrupt change in pressure of 2–4 cmH_2O and duration of five breaths was imposed on the subject by controlling the inspiratory pressure level of the ventilator. To estimate E, the change in inspiratory pressure was divided by the difference between the end-expiratory volume levels before and immediately after the pressure step. At least three estimations of E were performed before the application of each test protocol.

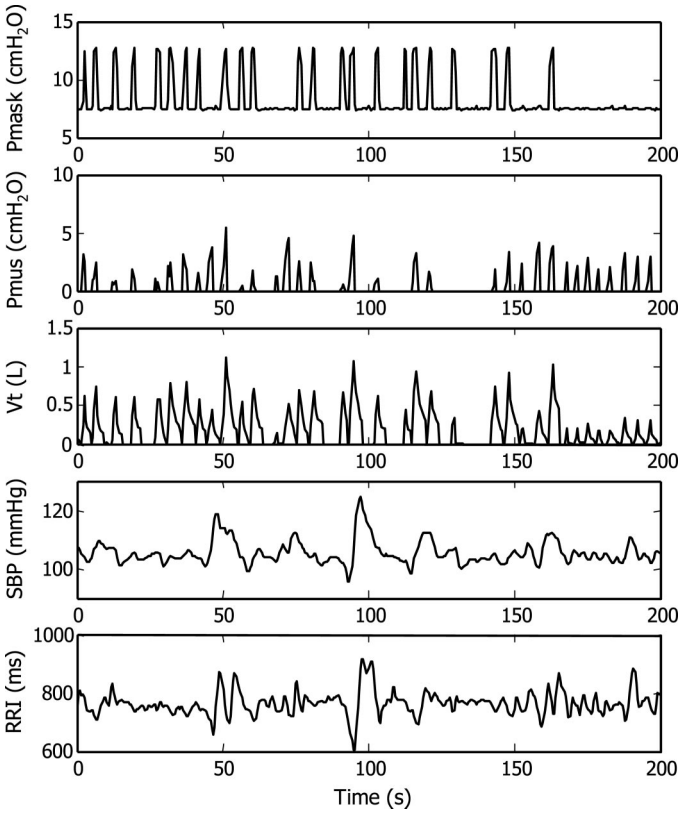

Fig. 2. Representative data segment showing estimated respiratory muscle pressure (P_{mus}) and measured tidal volume (V_T), systolic blood pressure (SBP), and RRI response of a patient with obstructive sleep apnea syndrome (OSAS) to the test protocol, in which positive airway pressure (P_{mask}) is applied randomly on a breath-to-breath basis during stage 2 sleep.

In the normal subjects during stage 2 sleep, R was found to be 6.21 ± 0.34 $cmH_2O \cdot s \cdot l^{-1}$, and E was 9.38 ± 0.69 cmH_2O/l. These values are consistent with normal respiratory mechanics (1, 25). However, R is higher and E slightly lower than the corresponding values reported by Meza et al. (26), who employed similar estimation methods in normal subjects during nonrandom eye movement (NREM) sleep. The discrepancy between our estimates and theirs is likely due to application of a smaller CPAP applied (2–3 cmH_2O) in our subjects. In contrast, in the study of Meza et al., the applied CPAP was titrated to a level (~5 cmH_2O) sufficient to minimize R during NREM sleep.

Statistical analysis. To facilitate statistical comparison, compact descriptors were derived from each model impulse response and its corresponding transfer function. These included the two measures of gain (IRM and DG) and the two measures of temporal behavior of the impulse response (delay and T_{peak}) described above (see *Model*). Each estimated parameter was subjected to two-way repeated-measures analysis of variance (with subject group as nonrepeated factor and sleep-wake state as repeated factor). Post hoc multiple pairwise comparisons (Student-Newman-Keuls test) were carried out if statistical significance ($P < 0.05$) was indicated.

RESULTS

Sample time series. A representative segment of data obtained from one of the OSAS patients is displayed in Fig. 2.

Table 1. *Measures of cardiovascular variability*

Parameter	Control			OSAS			*P*		
	Wakefulness	REM	Stage 2	Wakefulness	REM	Stage 2	Group	State	Group × state
				RRI variability					
RRI variance, ms^2	49.9±8.3	49.1±7.5	44.4±7.1	44.1±6.6	41.4±5.6	29.3±3.6	0.212	0.098	0.606
HFP_{RRI}, ms^2/Hz	242±66	327±151	503±188	320±100	96±24	110±35	0.147	0.488	0.022*
LFP_{RRI}, ms^2/Hz	313±103	208±80	206±73	274±96	213±99	101±21	0.597	0.153	0.739
				SBP variability					
SBP variance, $mmHg^2$	4.9±0.3	4.1±0.5	4.5±0.3	7.4±1.7	4.7±0.8	4.8±0.5	0.232	0.079	0.384
HFP_{SBP}, $mmHg^2/Hz$	1.99±0.71	0.94±0.49	1.23±0.45	6.57±2.94	1.77±0.71	2.50±0.72	0.143	0.043*	0.239
LFP_{SBP}, $mmHg^2/Hz$	2.82±0.66	1.50±0.29	1.86±0.41	6.84±2.95	3.49±1.28	3.99±1.38	0.034*	0.321	0.784
				DBP variability					
DBP variance, $mmHg^2$	3.5±0.7	2.7±0.3	2.8±0.3	5.7±1.4	4.1±0.5	3.4±0.4	0.059	0.108	0.508
HFP_{DBP}, $mmHg^2/Hz$	0.56±0.20	0.28±0.08	0.31±0.09	1.93±0.55	0.47±0.15	0.56±0.18	0.035*	0.002*	0.039*
LFP_{DBP}, $mmHg^2/Hz$	1.37±.37	1.46±0.52	1.40±0.60	4.04±1.31	2.86±0.98	3.91±2.56	0.043*	0.917	0.894

Values are means ± SE. OSAS, obstructive sleep apnea syndrome; REM, rapid eye movement sleep; RRI, R-R interval; HFP, high-frequency power; LFP, low-frequency power; SBP, systolic blood pressure; DBP, diastolic blood pressure. *$P < 0.05$.

CPAP of ~7 cmH_2O was applied throughout the duration of sleep. Figure 2 shows the randomly timed increases in inspiratory pressure delivered during the test procedure. The consequent variability imposed on the breathing pattern is quite evident in amplitude and duration. These respiratory variations, in turn, led to corresponding fluctuations in SBP and RRI. However, spontaneous fluctuations in SBP that were largely independent of the respiratory changes also occurred. Application of the random sequence of inspiratory pressure changes helped reduce the correlation between V and P_{mus}. For instance, at ~50 s, the applied inspiratory pressure occurred in synchrony with a large inspiratory effort (P_{mus}), whereas at ~130 s, there was no intrinsic respiratory drive during the ventilator-imposed breath, and from ~170–200 s, spontaneous breaths were generated by the subject in the absence of any applied inspiratory pressure.

Because the subjects were heavily instrumented, total sleep time was spent primarily in stage 2 and rapid eye movement (REM) sleep. Thus comparisons of the results were made across only three states: wakefulness, REM sleep, and NREM stage 2 sleep.

Measures of cardiovascular variability. Mean RRI was significantly lower in OSAS patients than in controls (799 ± 39 vs. 980 ± 44 ms in wakefulness, $P < 0.005$); in both groups, mean RRI increased from wakefulness to sleep ($P < 0.02$). Average minute ventilation during the test protocol in the control subjects was 9.0 ± 0.5, 7.4 ± 0.4, and 7.2 ± 0.3 l/min in wakefulness, REM sleep, and stage 2 sleep, respectively. The corresponding values for the OSAS group were 9.9 ± 0.6, 7.5 ± 0.4, and 6.8 ± 0.5 l/min, respectively. Thus, in both subject groups, ventilation decreased significantly ($P < 0.05$) from wakefulness to sleep.

The overall and spectral measures of heart rate and blood pressure variability are displayed in Table 1. There were no differences in RRI variance or low-frequency RRI power between groups or across states. However, high-frequency RRI power demonstrated a clear tendency during sleep to increase in controls but decrease in OSAS patients ($P < 0.03$). High-frequency SBP and DBP power decreased significantly from wakefulness to sleep ($P < 0.05$); this likely was due to the concomitant state-related reduction in ventilation. Low-frequency SBP power and DBP power were higher in OSAS patients than in controls in all states ($P < 0.05$).

Dynamics of the estimated model components. Sample traces of the estimated PSR impulse response [$h_{PSR}(t)$] corresponding to wakefulness, REM sleep, and stage 2 sleep in a control subject and one of the OSAS patients are shown in Fig. 3. In both individuals, the primary component of $h_{PSR}(t)$, which represents the vagal feedback from PSR, was a fast initial negative peak, indicating that pulmonary inflation increased heart rate reflexively, as has been reported previously (38). In wakefulness and sleep, $h_{PSR}(t)$ tended to be similar in magnitude in the OSAS patient and the control subject.

The estimated RCC impulse responses from the same control subject and OSAS patient are displayed in Fig. 3. Note that $h_{RCC}(t)$ was substantially smaller in magnitude in the OSAS patient than in the control subject during stage 2 and REM sleep. Also, $h_{RCC}(t)$ in the normal subject and OSAS patient assumed nonzero values before $t = 0$, indicating the previously observed tendency for changes in RRI to precede changes in respiratory effort (12, 27, 41). Both $h_{PSR}(t)$ and $h_{RCC}(t)$ assumed a biphasic shape, in which there was an initial large negative undershoot followed by a smaller positive overshoot. The initial negative dip is consistent with the well-accepted notion that the RSA consists of an acceleration of heart rate (or, equivalently, a reduction in RRI) during inspiration. The subsequent positive overshoot in the impulse response reflects the decrease in heart rate during expiration (25).

Sample traces of the estimated baroreflex impulse responses from the same control subject and OSAS patient are also displayed in Fig. 3. In this case, there was an initial large positive overshoot and a subsequent smaller negative undershoot, consistent with the notion that the net baroreflex response to an increase in blood pressure is a slowing of heart rate (or, equivalently, an increase in RRI). In all three states, $h_{ABR}(t)$ was substantially smaller in magnitude in the OSAS patient than in the control subject. In the OSAS patient and the control subject, there was a clear increase in the magnitude of $h_{ABR}(t)$ from wakefulness to stage 2 sleep.

Statistical comparison of model parameters. Table 2 displays the group-averaged results for all compact descriptors derived from the PSR, RCC, and ABR impulse responses; Fig.

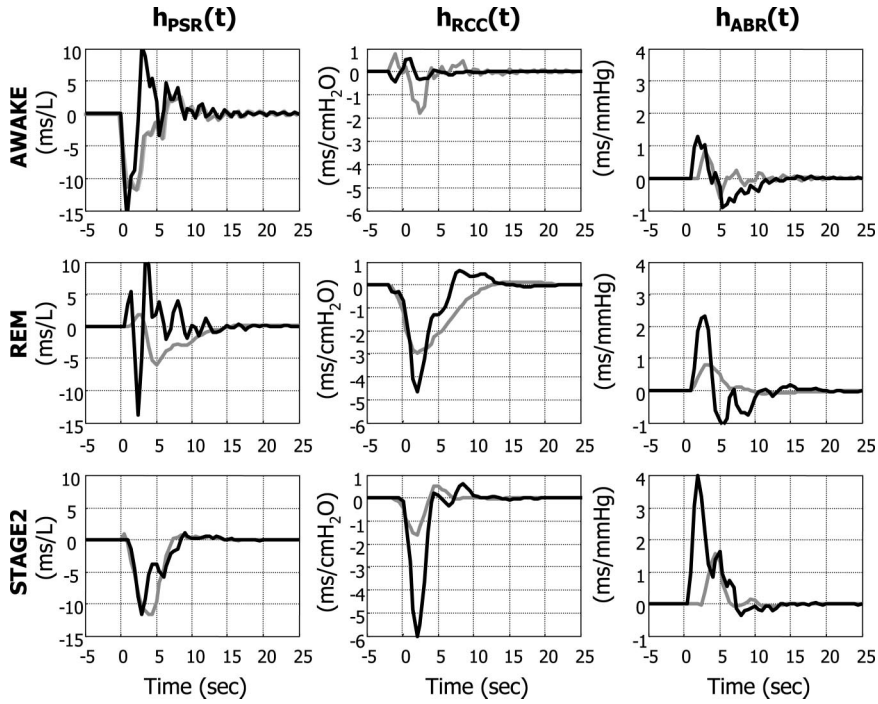

Fig. 3. Estimated impulse responses of the PSR (*left*), RCC (*middle*), and ABR (*right*) mechanisms of heart rate variability during wakefulness (awake), rapid eye movement (REM) sleep, and non-REM (stage 2) sleep in a representative control subject (solid traces) and an OSAS patient (shaded traces).

4 highlights those features that showed the greatest differences between subject groups or across sleep-wake states. Although there was a tendency for the descriptors of PSR gain to be lower in OSAS patients than in controls during sleep, these differences were not statistically significant. RCC gain increased from wakefulness to sleep ($P < 0.02$ for IRM_{RCC} and $P < 0.03$ for DG_{RCC}); however, this increase was clearly greater in the controls. RCC gain was lower in the OSAS patients than in the controls ($P < 0.04$ for IRM_{RCC} and $P < 0.02$ for DG_{RCC}), but the difference was largest in sleep. The time to peak of the RCC impulse response was significantly higher in OSAS in all states ($P < 0.03$). D_{RCC} assumed negative values, reflecting previous findings by others that changes in RRI precede changes in mechanical inspiration. There were no differences between subject groups or across sleep-wake states in D_{RCC}.

Both descriptors of ABR gain increased from wakefulness to sleep ($P < 0.004$ for IRM_{ABR} and $P < 0.02$ for DG_{ABR}). This increase tended to be higher in the controls. IRM_{ABR} was lower in the OSAS patients than in controls in all states ($P < 0.03$). The corresponding results for DG_{ABR} were more variable from subject to subject and, thus, failed marginally to attain statistical significance. There were no differences between subject groups or across sleep-wake states in the time course descriptors.

Relative component contributions to HRV. The average normalized mean square error for our model was 29.6% and 36.5% of total variance for the control and OSAS groups,

Table 2. *Model parameter estimates*

Parameter	Control			OSAS			*P*		
	Wakefulness	REM	Stage 2	Wakefulness	REM	Stage 2	Group	State	Group × state
				PSR					
IR magnitude, ms/l	24.4±5.3	37.1±8.5	35.2±5.9	21.8±4.7	17.9±2.7	20.9±4.5	0.078	0.356	0.089
Dynamic gain, ms/l	31.9±6.0	46.1±6.7	44.3±7.5	24.7±6.2	26.1±4.4	29.1±7.1	0.090	0.068	0.264
Latency, s	0.22±0.88	0.37±0.13	0.37±0.15	0.25±0.08	0.30±0.10	0.38±0.08	0.926	0.414	0.893
Time to peak, s	1.87±0.21	2.96±0.41	2.34±0.37	1.69±0.37	2.72±0.36	2.75±0.41	0.983	0.014*	0.596
				RCC					
IR magnitude, ms/cmH_2O	3.5±.5	5.8±1.1	5.4±0.8	2.8±0.4	3.3±0.3	3.4±0.5	0.038*	0.018*	0.105
Dynamic gain, ms/cmH_2O	6.5±0.9	10.4±1.9	9.5±1.4	4.6±0.7	5.2±0.7	5.7±0.9	0.012*	0.028*	0.164
Latency, s	−1.40±0.13	−1.34±0.23	−1.18±0.15	−1.38±0.15	−1.19±0.17	−1.44±0.13	0.829	0.732	0.458
Time to peak, s	2.50±0.18	2.31±0.23	2.25±0.18	2.88±0.22	2.69±0.20	2.64±0.16	0.026*	0.447	0.998
				ABR					
IR magnitude, ms/mmHg	2.5±0.3	5.6±1.5	6.2±1.0	1.8±0.4	2.9±0.8	2.5±0.7	0.027*	0.004*	0.079
Dynamic gain, ms/mmHg	2.7±0.5	4.6±1.5	4.9±0.9	1.8±0.4	2.7±0.5	2.5±0.6	0.079	0.012*	0.332
Latency, s	0.84±0.10	1.25±0.18	1.18±0.21	1.08±0.19	0.81±0.11	0.83±0.14	0.201	0.915	0.079
Time to peak, s	2.06±0.15	2.31±0.44	2.37±0.39	1.27±0.15	2.05±0.31	2.02±0.31	0.126	0.129	0.624

Values are means ± SE. PSR, pulmonary stretch reflex; IR, impulse response; RCC, respiratory-cardiac coupling; ABR, arterial baroreflex. *$P < 0.05$.

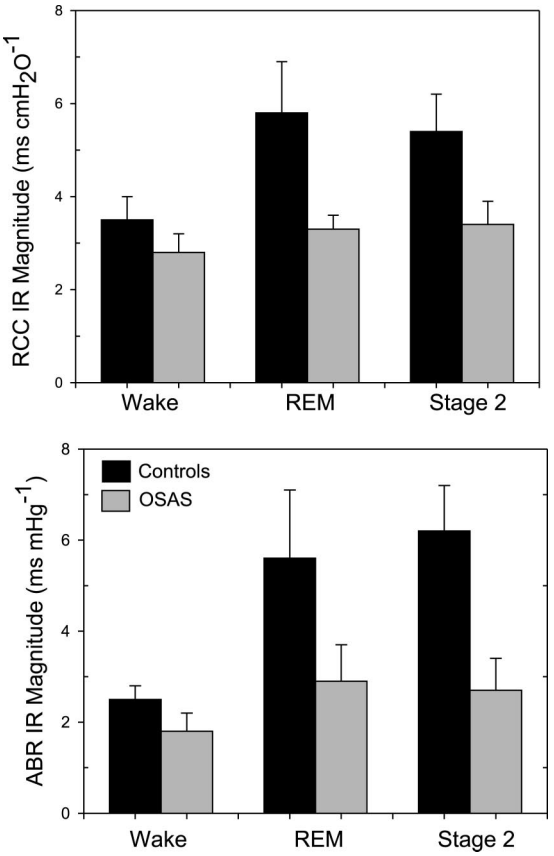

Fig. 4. Effects of OSAS and sleep-wake state on magnitude of RCC and ABR impulse responses.

respectively. This result indicates that our model was able to explain ~70% of the total variability of heart rate. Table 3 shows the relative percent contribution of each of the three components to overall predicted RRI variability. In normal subjects, the RCC mechanism accounted for the largest contribution to RRI variance, followed by ABR and PSR. In the OSAS group, contributions from RCC and ABR were more equally distributed. The PSR contribution remained consistently in the vicinity of 20% across sleep-wake states and between the two subject groups. On the other hand, the relative contribution from RCC was reduced ($P < 0.05$), whereas that from ABR was increased ($P < 0.02$), in OSAS. Furthermore, there was a significant trend for the ABR contribution to increase from wakefulness to sleep in both subject groups ($P < 0.03$).

DISCUSSION

Delineation of major components of HRV. Many previous studies have sought to determine the origin of RSA (2, 3, 35). However, most of these studies involved the use of anesthetized animal preparations and surgical or pharmacological techniques to eliminate one or more of the hypothesized mechanisms. In humans, because these highly invasive methods are clearly not applicable, ingenious experiments have been devised to delineate the different components of RSA. For example, in the study of Taha et al. (38), mechanical positive-pressure ventilation at high tidal volume was used to inhibit the central control of respiration (i.e., elimination of RCC output). In another study (30), phasic neck suction was applied to stimulate the ABRs at a prescribed frequency and, thus, enhance the output of the ABR mechanism. Although these techniques are noninvasive, they are nonetheless rather intrusive and impractical to apply in a clinical setting, particularly during sleep.

In contrast, the experimental protocol that we applied in the present study is relatively nonintrusive and generally well tolerated during sleep in normal subjects and patients with OSAS. Combining this experimental procedure with a model-based analysis allows us to computationally delineate the mechanisms of RSA. As well, the test protocol, in which positive airway pressure is introduced at randomly selected inspirations, serves as a means of perturbing the cardiorespiratory system over a broad range of frequencies. This facilitates the determination of the contributions of the three mechanisms over a dynamic range that extends beyond the band of respiratory frequencies (0.15–0.4 Hz) generally associated with RSA. Furthermore, broad-band stimulation has been shown to enhance the accuracy and reliability of parameter estimation (22). The random application of positive airway pressure also is useful for a third purpose. During spontaneous breathing, P_{mus} is strongly correlated with V, because a breath with stronger respiratory drive would generally produce a larger tidal volume; under such conditions, it would not be possible to distinguish the contributions of PSR from those of RCC. However, the introduction of a randomly modulated ventilatory sequence acts to decorrelate P_{mus} and V, because a large tidal volume can also result from a breath with weak intrinsic respiratory drive that has been bolstered by the ventilatory assist (Fig. 2).

An important feature of this study is the use of a mathematical model that allows the contributions from the three inputs to be delineated. Although respiration and blood pressure are treated as though they are mutually independent inputs, these variables and heart rate are part of a larger closed-loop control system (Fig. 1). However, delays in this closed-loop system allow us to computationally partition the feedforward and feedback portions, so that each portion of the system can be treated as though it is operating under open-loop conditions (20). For instance, in the baroreflex portion of the closed-loop system, present changes in RRI are constrained in the mathe-

Table 3. *Relative component contributions to heart rate variability*

Model Component	Control			OSAS			*P*		
	Wakefulness	REM	Stage 2	Wakefulness	REM	Stage 2	Group	State	Group × state
PSR	21.5±5.3	18.4±2.4	20.5±4.0	20.1±5.0	14.9±2.9	18.1±2.5	0.540	0.548	0.961
RCC	61.4±5.5	47.1±6.4	46.7±4.9	48.7±6.5	39.8±6.3	36.7±5.2	0.048*	0.060	0.902
ABR	17.1±3.1	34.5±7.1	32.9±4.8	31.1±6.7	45.4±7.0	45.2±5.3	0.012*	0.022*	0.965

Values are means ± SE expressed as percentages. *$P < 0.05$.

matical model to be influenced by only past, but not present or future, fluctuations of blood pressure. This imposed constraint (termed causality in systems engineering terminology) forces the estimation scheme to converge toward a solution that reflects the effect of blood pressure on RRI (i.e., the baroreflex) rather than one that reflects the effects of RRI on blood pressure (i.e., the feedforward component). This approach of "temporal delineation" can only be applied by employing a model that has been formulated in the time domain. In contrast, frequency-domain methods, such as techniques that employ cross-spectral analysis, do not allow the implementation of causality constraints. The application of this type of computational approach to cardiovascular control has appeared in publications by other researchers (12, 27, 41).

Effects of CPAP. During sleep in the OSAS patients, CPAP was applied at individually prescribed levels to ensure upper airway patency throughout the test procedure. We believe that this was an important part of the experimental procedure, because it enabled us to perform a comparative assessment of autonomic control between normal subjects and patients with OSAS across different sleep-wake states. Application of CPAP also ensured that all individuals could be studied under relatively similar patterns of respiration in stable stages of REM and NREM sleep. In contrast, previous investigations of autonomic control in OSAS during sleep were carried out under uncontrolled conditions, in which the episodes of obstructive apnea were associated with profound swings in sympathetic and parasympathetic activity as well as transient state changes (19, 39). Large swings in respiration and cardiovascular variables can lead to severe distortions of the HRV and blood pressure variability spectra and, thus, contribute to interpretational difficulties if these spectral measures are used for making inferences about autonomic function (21).

On the other hand, CPAP application in the OSAS patients during sleep may have led inevitably to some confounding influences. For example, in subjects with normal heart function, acute application of CPAP is known to decrease left ventricular preload more than left ventricular afterload, leading to a reduction in cardiac output (13). However, our OSAS patients did not show any change in mean SBP or DBP during sleep relative to wakefulness when only minimal CPAP was applied. Furthermore, CPAP is likely to have increased lung volume, which is known to increase vagal activity and reduce sympathetic drive (11). Therefore, our technique is likely to have underestimated the extent of autonomic abnormality in the OSAS patients during sleep.

Dynamics of the estimated model components. The forms of the estimated impulse responses corresponding to the three mechanisms appear to be consistent with the underlying physiology. The PSR impulse response, which represents the vagal feedback from PSR, shows a fast initial negative peak and a delay between V and RRI, indicating that pulmonary inflation increases heart rate reflexly but with some delay after the initiation of inspiration, as has been reported previously (37). The RCC impulse response, which represents the central component of RSA, shows a fast initial negative peak and a lead (negative delay) between heart rate and P_{mus}, reflecting an increase in heart rate during inspiratory effort. The ABR impulse response increases initially to positive values, reflecting a very rapid decrease in heart rate (or, equivalently, increase in RRI) in response to an increase in blood pressure. All three impulse responses showed time courses that decayed within 15 s. The rapidity of the dynamic behavior suggests that all three components of HRV are mediated primarily by the parasympathetic system.

Effects of OSAS and sleep state on HRV components. The main finding in this study is that, in wakefulness and sleep, RCC and ABR gains were reduced in patients with OSAS compared with normal subjects. The second major finding is that, in both subject groups, ABR and RCC gains increased from wakefulness to sleep. These results are consistent with the fact that sympathetic tone is chronically elevated in patients with OSAS (36). Elevated sympathetic tone, such as in patients with congestive heart failure (36) or postmyocardial infarction (15), is associated with diminished baroreflex function. Increased sympathetic tone induced by mental stress is also known to reduce the parasympathetic influence on heart rate regulation (9). For example, voluntary override of the spontaneous respiratory pattern generator by controlled breathing has been shown to decrease high-frequency power RRI substantially in normal subjects (29). On the other hand, our results also show that sleep leads to increases in RCC and ABR gains, consistent with the notion that parasympathetic tone becomes elevated during sleep (24).

In contrast, there were no significant differences in PSR gain between normal subjects and OSAS patients; nor did either group demonstrate any dependence of PSR gain on sleep-wake state. There was substantial interindividual variability within each group in the PSR gain estimates (see sizes of standard errors in Table 2), and this may have obscured any real intergroup differences. The relative contribution of PSR to overall HRV was also uninfluenced by subject group or sleep-wake state. These findings suggest that the PSR mechanism is little affected by differences in sympathetic tone resulting from disease or differences in parasympathetic tone arising from changes in sleep-wake state. Why this should be so remains unclear and requires further testing using a larger pool of subjects. A further finding is that, in OSAS patients and normal subjects, PSR contributes the least of all three mechanisms to overall HRV. Similarly, previous studies in humans have shown that the contribution of the lung vagal reflexes to RSA is small (2, 3, 35) but nonnegligible (38).

A potential limitation of this study is that although we categorized "moderate-to-severe" OSAS as a single group, disease severity covered a broad range of apnea-hypopnea index values (from 21 to 88). It could be argued that a portion of the interindividual variability found in the OSAS group might well have been related to differences in disease severity. On the other hand, two observations make this hypothesis unlikely. *1*) The interindividual variability (as represented by the standard errors of the estimated parameters in Table 2) in the control group was as large as the variability in the OSAS group. *2*) We computed linear correlation coefficients between each parameter and apnea-hypopnea index. No significant correlations were found.

Estimation of baroreflex gain: comparison with previous studies. In our previous study in which we employed a dual-input model, we also found that ABR gain was significantly lower in OSAS patients than in normal subjects across all states, but the difference was largest during sleep. These amplitudes increased almost twofold in sleep vs. wakefulness in normal subjects but were less affected by state changes in

OSAS. The inclusion of a third input (i.e., P_{mus}) in the present model did not significantly alter our estimates of baroreflex gain from the same datasets. The similarity of our present and previous estimates of ABR gain validates our prior assumption that the test protocol produces input sequences (i.e., P_{mus}, V, and SBP time series) that are not strongly correlated with one another.

We previously showed that our model-based estimates of ABR gain correlate significantly with baroreflex sensitivity calculated using conventional methods, such as the "sequence technique" and the bolus technique (7). These conventional methods, however, do not take into account the contribution of respiration to the fluctuations in RRI. A recent study has shown that excluding the effect of respiration on RRI can lead to the introduction of a significant amount of bias into the computation of baroreflex sensitivity (23). In our model-based approach, the component of the RRI fluctuations linearly correlated to respiration is removed before the remaining values are related to SBP fluctuations for the estimation of baroreflex gain. As well, our model makes the more realistic assumption that baroreflex action is associated with dynamic characteristics (e.g., response time); the aforementioned pharmacological and sequence techniques do not take into account baroreflex dynamics.

In conclusion, the model proposed in this study allows for the independent quantitative characterization of the three main autonomically mediated mechanisms involved in control of heart rate: vagal feedback from the PSR, central coupling between the respiratory and cardioregulatory centers, and the ABR. This can be achieved by using the model to analyze the cardiovascular responses to a test protocol in which positive airway pressure is applied in the form of a randomized sequence of breaths. The test protocol is nonintrusive and is reasonably well tolerated during sleep. Our results show that the adverse autonomic effects of OSAS include impairment of baroreflex sensitivity and the central mechanism linking respiratory drive with heart rate regulation. However, the component of RSA that is mediated by lung vagal feedback remains intact in OSAS. In normal subjects and OSAS patients, this third mechanism of HRV is relatively unaffected by changes in sleep-wake state, whereas the other two components demonstrate an increase in gain during sleep. Future studies could include the extension of the model to incorporate other potentially important factors affecting HRV, such as the contributions of the cardiopulmonary receptors and the chemoreflexes. As well, a determination of the relative impairment of these different contributions to HRV in patients with less severe manifestations of the disease could yield important insights into the long-term development of autonomic abnormality in OSAS.

GRANTS

This study was supported by National Institutes of Health Grants HL-58725, EB-001978, and M01 RR-43.

REFERENCES

1. **Agostoni E and Mead J.** Statics of the respiratory system. In: *Handbook of Physiology. Respiration*. Washington, DC: Am. Physiol. Soc., 1964, sect. 3, vol. I, chapt. 13, p. 387–409.
2. **Anrep GV, Pascual W, and Roessler R.** Respiratory variation of the heart rate. I. The reflex mechanism of the respiratory arrhythmia. *Proc R Soc Lond B Biol Sci* 119: 191–217, 1936.
3. **Anrep GV, Pascual W, and Roessler R.** Respiratory variation of the heart rate. II. The central mechanism of the respiratory arrhythmia and the inter-relation between the central and the reflex mechanisms. *Proc R Soc Lond B Biol Sci* 119: 218–232, 1936.
4. **Baselli G, Cerutti S, Civardi S, Malliani A, and Pagani M.** Cardiovascular variability signals: towards the identification of a closed-loop model of the neural control mechanisms. *IEEE Trans Biomed Eng* 35: 1033–1046, 1988.
5. **Baydur A.** Decay of inspiratory muscle pressure during expiration in anesthetized kyphoscoliosis patients. *J Appl Physiol* 72: 712–720, 1992.
6. **Behrakis PK, Higgs BD, Baydur A, Zin WA, and Milic Emili J.** Respiratory mechanics during halothane anesthesia and anesthesia-paralysis in humans. *J Appl Physiol* 55: 1085–1092, 1983.
7. **Belozeroff V, Berry RB, and Khoo MC.** Model-based assessment of autonomic control in obstructive sleep apnea syndrome. *Sleep* 26: 65–73, 2003.
8. **Berger RD, Akselrod S, Gordon D, and Cohen RJ.** An efficient algorithm for spectral analysis of heart rate variability. *IEEE Trans Biomed Eng* 33: 900–904, 1986.
9. **Berntson GG, Bigger JT Jr, Eckberg DL, Grossman P, Kaufmann PG, Malik M, Nagaraja HN, Porges SW, Saul JP, Stone PH, and van der Molen MW.** Heart rate variability: origins, methods, and interpretive caveats. *Psychophysiology* 34: 623–648, 1997.
10. **Brooks D, Horner RL, Kozar LF, Render-Teixeira CL, and Phillipson EA.** Obstructive sleep apnea as a cause of systemic hypertension. Evidence from a canine model. *J Clin Invest* 99: 106–109, 1997.
11. **Butler GC, Naughton MT, Rahman MA, Bradley TD, and Floras JS.** Continuous positive airway pressure increases heart rate variability in congestive heart failure. *J Am Coll Cardiol* 25: 672–679, 1995.
12. **Chon KH, Mullen TJ, and Cohen RJ.** A dual-input nonlinear system analysis of autonomic modulation of heart rate. *IEEE Trans Biomed Eng* 43: 530–544, 1996.
13. **De Hoyos A, Liu PP, Benard DC, and Bradley TD.** Haemodynamic effects of continuous positive airway pressure in humans with normal and impaired left ventricular function. *Clin Sci (Lond)* 88: 173–178, 1995.
14. **Eckberg D.** Respiratory sinus arrhythmia and other human cardiovascular neural periodicities. In: *Regulation of Breathing* (2nd ed.), edited by Dempsey JA and Pack AI. New York: Dekker, 1995, p. 669–740.
15. **Farrell TG, Odemuyiwa O, Bashir Y, Cripps TR, Malik M, Ward DE, and Camm AJ.** Prognostic value of baroreflex sensitivity testing after acute myocardial infarction. *Br Heart J* 67: 129–137, 1992.
16. **Francis DP, Coats AJ, and Ponikowski P.** Chemoreflex-baroreflex interactions in cardiovascular disease. In: *Sleep Apnea: Implications in Cardiovascular and Cerebrovascular Disease*, edited by Bradley TD and Floras JS. New York: Dekker, 2000, p. 33–60.
17. **Jo JA, Blasi A, Valladares E, Juarez R, Baydur A, and Khoo MC.** Model-based assessment of autonomic control in obstructive sleep apnea syndrome during sleep. *Am J Respir Crit Care Med* 167: 128–136, 2003.
18. **Katona PG, Poitras JW, Barnett GO, and Terry BS.** Cardiac vagal efferent activity and heart period in the carotid sinus reflex. *Am J Physiol* 218: 1030–1037, 1970.
19. **Keyl C, Lemberger P, Dambacher M, Geisler P, Hochmuth K, and Frey AW.** Heart rate variability in patients with obstructive sleep apnea. *Clin Sci (Lond)* 91 *Suppl*: 56–57, 1996.
20. **Khoo MC.** *Physiological Control Systems: Analysis, Simulation and Estimation*. Piscataway, NJ: IEEE Press, 2000.
21. **Khoo MC, Kim TS, and Berry RB.** Spectral indices of cardiac autonomic function in obstructive sleep apnea. *Sleep* 22: 443–451, 1999.
22. **Kim TS and Khoo MC.** Estimation of cardiorespiratory transfer under spontaneous breathing conditions: a theoretical study. *Am J Physiol Heart Circ Physiol* 273: H1012–H1023, 1997.
23. **Lucini D, Porta A, Milani O, Baselli G, and Pagani M.** Assessment of arterial and cardiopulmonary baroreflex gains from simultaneous recordings of spontaneous cardiovascular and respiratory variability. *J Hypertens* 18: 281–286, 2000.
24. **Mancia G and Mark AL.** Arterial baroreflexes in humans. In: *Handbook of Physiology. The Cardiovascular System. Peripheral Circulation and Organ Blood Flow*. Bethesda, MD: Am. Physiol. Soc., 1983, sect. 3, vol. III, pt. 2, Chapt. 20, p. 755–793.

25. **Mead J and Agostoni E.** Dynamics of breathing. In: *Handbook of Physiology. Respiration.* Washington, DC: Am. Physiol. Soc., 1964, sect. 3, vol. I, chapt. 14, p. 411–427.
26. **Meza S, Giannouli E, and Younes M.** Control of breathing during sleep assessed by proportional assist ventilation. *J Appl Physiol* 84: 3–12, 1998.
27. **Mullen TJ, Appel ML, Mukkamala R, Mathias JM, and Cohen RJ.** System identification of closed-loop cardiovascular control: effects of posture and autonomic blockade. *Am J Physiol Heart Circ Physiol* 272: H448–H461, 1997.
28. **Narkiewicz K, Montano N, Cogliati C, van de Borne PJ, Dyken ME, and Somers VK.** Altered cardiovascular variability in obstructive sleep apnea. *Circulation* 98: 1071–1077, 1998.
29. **Patwardhan AR, Vallurupalli S, Evans JM, Bruce EN, and Knapp CF.** Override of spontaneous respiratory pattern generator reduces cardiovascular parasympathetic influence. *J Appl Physiol* 79: 1048–1054, 1995.
30. **Piepoli M, Sleight P, Leuzzi S, Valle F, Spadacini G, Passino C, Johnston J, and Bernardi L.** Origin of respiratory sinus arrhythmia in conscious humans. An important role for arterial carotid baroreceptors. *Circulation* 95: 1813–1821, 1997.
31. **Rechtschaffen A and Kales R.** *A Manual of Standardized Terminology, Techniques and Scoring System for Sleep Stages of Human Subjects*. Los Angeles, CA: BIS/BRI, UCLA, 1968.
32. **Rissanen J.** Estimation of structure by minimum description length. *Circ Syst Sig Proc* 1: 395–406, 1982.
33. **Roux F, D'Ambrosio C, and Mohsenin V.** Sleep-related breathing disorders and cardiovascular disease. *Am J Med* 108: 396–402, 2000.
34. **Shahar E, Whitney CW, Redline S, Lee ET, Newman AB, Javier NF, O'Connor GT, Boland LL, Schwartz JE, and Samet JM.** Sleep-disordered breathing and cardiovascular disease: cross-sectional results of the Sleep Heart Health Study. *Am J Respir Crit Care Med* 163: 19–25, 2001.
35. **Shykoff BE, Naqvi SS, Menon AS, and Slutsky AS.** Respiratory sinus arrhythmia in dogs. Effects of phasic afferents and chemostimulation. *J Clin Invest* 87: 1621–1627, 1991.
36. **Somers VK, Dyken ME, Clary MP, and Abboud FM.** Sympathetic neural mechanisms in obstructive sleep apnea. *J Clin Invest* 96: 1897–1904, 1995.
37. **St. Croix CM, Satoh M, Morgan BJ, Skatrud JB, and Dempsey JA.** Role of respiratory motor output in within-breath modulation of muscle sympathetic nerve activity in humans. *Circ Res* 85: 457–469, 1999.
38. **Taha BH, Simon PM, Dempsey JA, Skatrud JB, and Iber C.** Respiratory sinus arrhythmia in humans: an obligatory role for vagal feedback from the lungs. *J Appl Physiol* 78: 638–645, 1995.
39. **Vanninen E, Tuunainen A, Kansanen M, Uusitupa M, and Lansimies E.** Cardiac sympathovagal balance during sleep apnea episodes. *Clin Physiol* 16: 209–216, 1996.
40. **Wiklund U, Olofsson BO, Franklin K, Blom H, Bjerle P, and Niklasson U.** Autonomic cardiovascular regulation in patients with obstructive sleep apnoea: a study based on spectral analysis of heart rate variability. *Clin Physiol* 20: 234–241, 2000.
41. **Yana K, Saul JP, Berger RD, Perrott MH, and Cohen RJ.** A time domain approach for the fluctuation analysis of heart rate related to instantaneous lung volume. *IEEE Trans Biomed Eng* 40: 74–81, 1993.
42. **Zwillich CW.** Sleep apnoea and autonomic function. *Thorax* 53, *Suppl* 3: S20–S24, 1998.